DEVELOPMENT OF A CERTIFICATION PROCEDURE FOR NUMERICAL PEDESTRIAN MODELS

Corina Klug, Florian Feist, Bernd Schneider, Wolfgang Sinz
Graz University of Technology
Austria

James Ellway, Michiel van Ratingen
Euro NCAP
Belgium

Paper Number 19-0310

ABSTRACT

In the Euro NCAP testing of deployable pedestrian protection systems (i.e. active bonnets and airbags), head impact time (HIT), wrap around distance and bonnet deflection due to body loading are assessed by means of simulations with numerical pedestrian models. The aim of this study was to define requirements for numerical pedestrian models and simulation setups to ensure comparable performance of models and simulation results. These requirements were summarized in a certification procedure which focuses on the pedestrian's kinematics that are important for the Euro NCAP assessment. Twelve different institutions (academia and industry) applied a harmonised pedestrian simulation protocol, which was established within a previous study. Numerical pedestrian models in the stature of the 50th percentile male (all applicable for the assessment of deployable systems until 2017) were impacted with four differently shaped generic vehicle models at three different collision speeds according to the protocol. Trajectories, contact forces and HITs were evaluated. Finally, 18 full data sets including the 12 load cases were available covering different Human Body Models and Humanoid Multibody Models in four different FE codes. Reference values, corridors and tolerances for the certification procedure were derived, based on identified consistent results. Comparable behaviour was observed for the majority of pedestrian models. However, a small number of simulations showed clearly outlying behaviour in terms of HITs, trajectories and contact forces. The consistent models were within a range of +3.5% and -7% throughout all load cases. Corridors for the z- and x- trajectories as a function of time were developed for the head centre of gravity, T12 and the centre of acetabuli for each load case. Furthermore, corridors for the contact forces between pedestrian model and generic vehicle model were established. The developed certification procedure ensures that a specific pedestrian model within a specific environment, solver version and specific simulation settings gives comparable kinematic results relevant for the assessment of deployable systems. Inconsistent pedestrian models, incompatibilities with control settings and user errors can be identified and sorted out. The procedure was implemented in the Euro NCAP Technical Bulletin 24 and has been in force since January 2018.

INTRODUCTION

The Euro NCAP (European New Car Assessment Programme) assessment of deployable systems (i.e. active bonnets) represents the first application of Human Body Models within a consumer information safety rating. The timing and the impact location of the head are essential information for the assessment of deployable systems such as active pop-up bonnets. The system must detect the pedestrian and deploy rapidly enough before the head contacts the bonnet. Furthermore, evidence must be provided showing that the bonnet and the support structures are sufficiently stiff to ensure that the additional clearance has not already been significantly compromised due to the body load prior to the head impact.
These parameters cannot be assessed using the conventional subsystem impactors. Therefore, input from simulations is needed: A hybrid approach has been adopted by Euro NCAP for the assessment of deployable systems, which covers virtual simulations with pedestrian models, and physical tests with pedestrian subsystem impactors. The simulations with the pedestrian models are carried out to derive inputs for the subsequent physical tests with headform impactors. The virtual tests cover multiple collision speeds and pedestrian statures: Firstly, the head impact location (*WAD*) and Head Impact Time (*HIT*) for several pedestrian sizes are determined to assess whether the system can be fully deployed by the time of head impact for the most critical pedestrian stature. Secondly, the pedestrian size that is hardest for the sensor system to detect can be determined by means of performing simulations as an alternative to physical tests and to select appropriate test tools, which is in almost all cases the 6yo stature. Finally, the bonnet deflection due to the bonnet loading is derived from the

simulations with pedestrian models to prove that the head protection is not compromised by a collapse of the bonnet. Based on the simulation results, physical tests are performed when the active bonnet is deployed, undeployed, or deploying. Conventional headform impactors are used, and the measured linear accelerations are applied to derive the Head Injury Criterion (*HIC*) values upon which the final scores are based. [1]
The virtual pedestrian simulations described above must be carried out at varying collision speeds with several sizes of the pedestrian models (6yo, 5th, 50th, 95th) but Euro NCAP does not specify the type of Human Body Model [1]. Ensuring comparability of simulation results for this application, however, is of great importance as differences between simulated HIT values and the total response times (TRT= sensing time + deployment time) of the active bonnets are often very close. This is shown in Figure 1, where results submitted to Euro NCAP are shown, which were used for the assessment of deployable systems. The HIT values of the simulations with different pedestrian statures are overlaid and compared with the TRT values. HIT values are only provided for the statures where head contact with the bonnet occurred, which is why there are fewer values for the 95th model (green bars), than values representing the other statures. The 6yo model was not contacting the bonnet in only two of the 47 analysed dossiers. In six cases the TRT was higher than the TRT of the smallest pedestrian model that impacts the bonnet. The average relative positive deviation between the HIT of the smallest stature that was impacting the bonnet and the TRT was 15.6% and the median relative deviation was 11.7% (for the 41 results in which the HIT was ≤TRT). In five of the dossiers the HIT value of the 6yo model was even equal to the TRT.

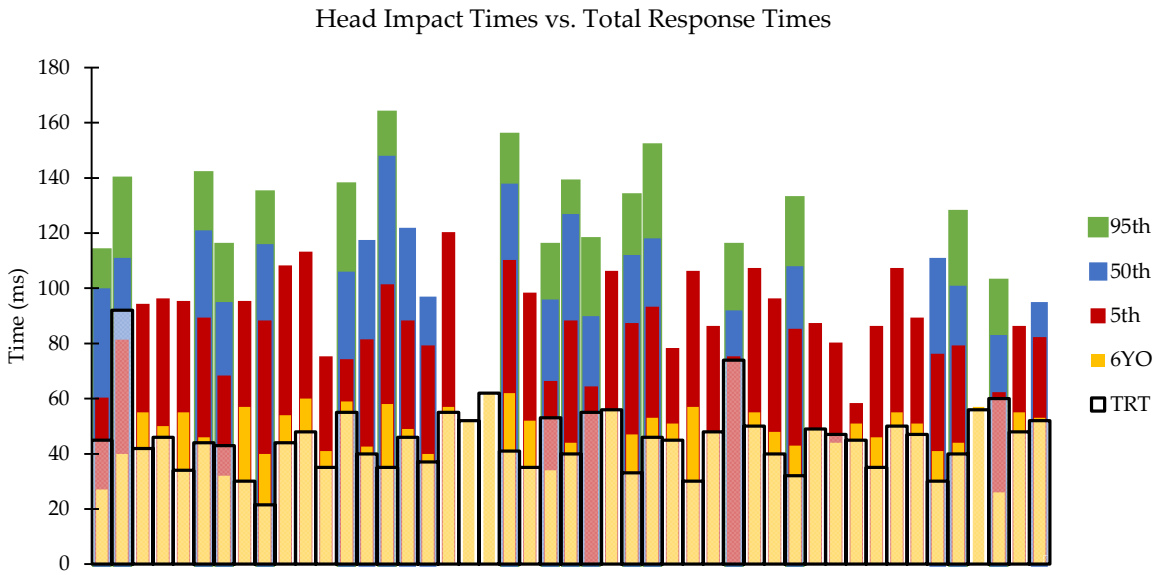

Figure 1: Head Impact Times of different pedestrian sizes overlaid and compared to Total Response Times of active bonnets based on results submitted to Euro NCAP from 2010-2018 (n=47).

Prior to 2018, all pedestrian models listed in Technical Bulletin 13 [2] could be applied for the virtual part of the assessment [1]. The list of models did not cover the effects of altering simulation settings and was difficult to maintain, because HBMs are continuously revised. Furthermore, the protocol did not include all details for the HBM simulations (e.g. open arm and torso posture, open contact settings), although these boundary conditions have been shown to have an effect in several studies [3–9].
As an alternative to a list of models, a certification procedure for virtual pedestrian models was established within the current study. The idea of the certification procedure is that simulations performed by a specific user with a specific HBM using a specific FE solver and specific control settings can be compared to a set of reference simulations. This will help to ensure comparability of the simulation results. For the final assessment simulations only the vehicle model is exchanged (using the detailed serial FE vehicle model to be assessed instead of the generic vehicle model), while anything else (solver, control settings, pedestrian model, contact settings) remains unchanged.
The aim of the study was to define corridors and tolerances for a certification procedure based on consistent reference results from state-of-the-art HBMs.

METHOD

Simulation setups

Generic vehicle (GV) models were applied as impact structures. The GV models were defined such that were easily transferrable to other codes and were thus applicable for comparison of HBMs in different codes (LS-

Dyna, VPS, Radioss and Abaqus). The model structure and geometry is explained in detail in [10]. Four different shapes of the models were established, representing the geometry of an FCR (family car), an MPV (Multipurpose Vehicle), an RDS (roadster) and an SUV (sport utility vehicle). The LS-DYNA version of the GV models was translated into the other FE codes by the FE code houses (ESI Group, Altair and Dassault Systèmes). The simulation protocol was developed with THUMS v4.02 and the simplified GHBMC pedestrian model in LS-DYNA and was published previously [10,11]. Twelve load cases were defined, in which the pedestrian is impacted with the four GV models at three different collision speeds (30, 40 and 50 km/h) in a specified reference posture [10] mimicking a natural walking position.

Analysed outputs

Sensors were implemented in the HBMs at selected reference points for the evaluation of trajectories:

- the head centre of gravity (HC)
- the centre (average of all nodal coordinates) of the vertebral body of C7 and T12
- the midpoint of the left and right centre of the acetabulum (AC)

A detailed description of the reference point sensor locations can be found in the Appendix (Table 2), allowing different users to position comparable sensor positioning in multiple HBMs. The sensors were connected with the structure using the keyword *CONSTRAINED_INTERPOLATE in LS-DYNA. In the other FE software packages, keywords with the same algorithm were identified and are provided in Table 3 in the Appendix.

For the evaluation of the trajectories, the x-displacement of the vehicle was subtracted from the x coordinates of the sensors (stationary vehicle view in local vehicle coordinate system) according to Figure 7. Contact forces and node histories were outputted every 0.1 ms. Unfiltered curves were used.

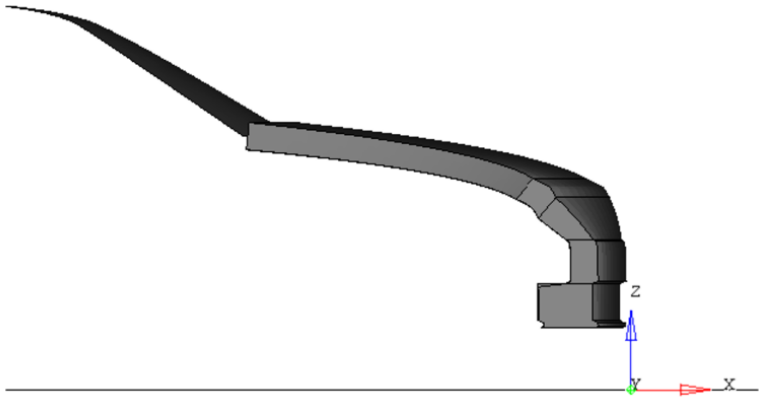

Figure 2: Coordinate system of the vehicle as applied in this study (x=0 at foremost point on vehicle front).

The kinematic assessment placed a focus on the head, as this is most relevant for the assessment of active bonnets.

The *HIT* was defined as the time from the first increase in the bumper contact force (*C*) until the first increase in the contact force between the head and vehicle (*H*), as shown in Figure 3 and described in Equation 1.

$$HIT\ [ms] = H - C \qquad \text{(Equation 1)}$$

The acceleration measured within the head CoG was also used to double-check the result, as shown in Figure 3. To determine *C,* only the contact between the lower extremities and bumper was considered (as this is also used as a trigger for active bonnets). A first contact between upper extremities and bumper was ignored.

The contact forces were separated by body region and contact surface. For the comparison between the models, the resultant total contact force between HBM and GV was used. The times of all contact forces were offset with the value C (time of first contact = 0).

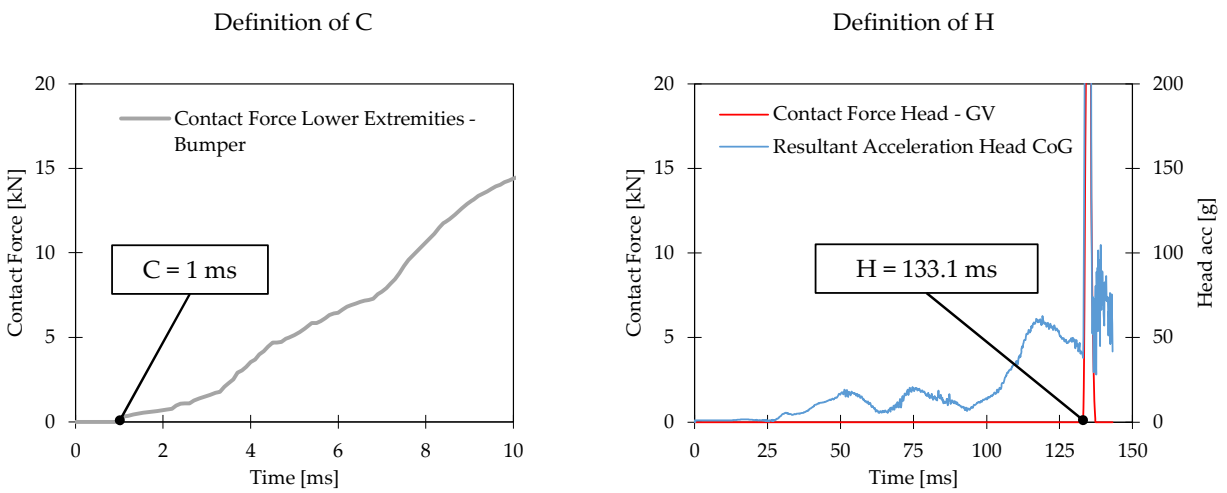

Figure 3: Example for the calculation of HIT based on H and C.

Dataset

A number of institutions from around the world run simulations according to the protocol [10] using the GV models and have provided their results. These are Audi AG, BMW Group, Daimler AG, ESI Group, HongIk University, Jaguar Land Rover, Honda R&D, Japan Automobile Manufacturers Association (JAMA) and Japan Automobile Research Institute (JARI), Nissan Motor Company, Siemens Industry Software and Services B.V. (formerly known as Tass International), Subaru Corporation and Wake Forest University. The results from the following pedestrian models (HBMs and multibody humanoid models) were included in the final dataset (random order):

- GHBMC simplified pedestrian model:
  - VPS version without fracture mode (two different institutions)
  - RADIOSS version without fracture mode
  - LS-DYNA with fracture mode (v1.4.5 and v1.4.3)
- THUMS:
  - THUMS v4.02 in LS-DYNA without fracture mode (two different institutions)
  - THUMS v4 in VPS without fracture mode
  - THUMS TUC in LS-DYNA without fracture mode
  - THUMS-D in LS-DYNA without fracture mode
  - THUMS v3 in Abaqus without fracture mode
- JAMA Pedestrian Model (HBM) in VPS with and without fracture mode
- Honda HBM in VPS without fracture mode
- Simcenter Madymo™ pedestrian models (multibody humanoid model) coupled with LS-DYNA (two different institutions)
- JLR humanoid FE model in LS-DYNA
- ESI PED 50 humanoid FE model in VPS

The results were anonymised and named as Model 01 to Model 18. All of the above listed models were included in the list of Euro NCAP TB013 and were, therefore, applicable for Euro NCAP assessment of deployable systems until December 2017.

The results from different models at different institutions and in different FE software packages were grouped into “consistent” and “inconsistent” results based on qualitative comparisons of the curves and the results of the statistical analyses.

Boxplots were used to identify outliers and to compare the HITs. Outliers were defined as points beyond the 1.5 interquartile ranges ($IQR = Q3 - Q1$) from the median value (shown as a whisker in the diagrams). Reference values and tolerances for head impact times were derived.

Corridors were derived for trajectories for the locations of HC, T12 and AC based on the consistent results. The median, minimum and maximum values for each coordinate were derived from all consistent results every 0.1 ms.

Additionally, corridors for the total resultant contact force between HBM and GV were defined based on the minimum and maximum value of the consistent results (again every 0.1 ms).

RESULTS

Eighteen different dossiers of results were available for the subsequent analysis, again using the names Model 01 to Model 18. In the case of Model 5, no results of the impacts with 30 km/h were provided. The dossier was complete for all other models and included all twelve load cases. In the first step, outliers were identified and removed from the dataset. Corridors for the trajectories, displacements and contact forces were specified based on consistent results. Furthermore, reference values and tolerances for *HIT*s were defined for the final certification procedure.

Head Impact Time

The head impact times resulting from the eighteen different pedestrian simulations with varying pedestrian models in four different codes are shown in Figure 4. Boxplots were created to identify outliers in the datasets. The boxes show the 1st quartile (*Q1*), median value and 3rd quartile (*Q3*). The whiskers represent the highest or lowest value within the 1.5 *IQR*. The cross indicates the mean value for each load case. As the distributions were not symmetric, the median values together with quartiles were found to be more useful than the mean values with standard deviation.

Six outlying results were identified and are shown as circles in the figure: Results from Pedestrian Models 2, 5, 6, 11, 12 and 15 did not fall within the 1.5 *IQR* for at least one load case.

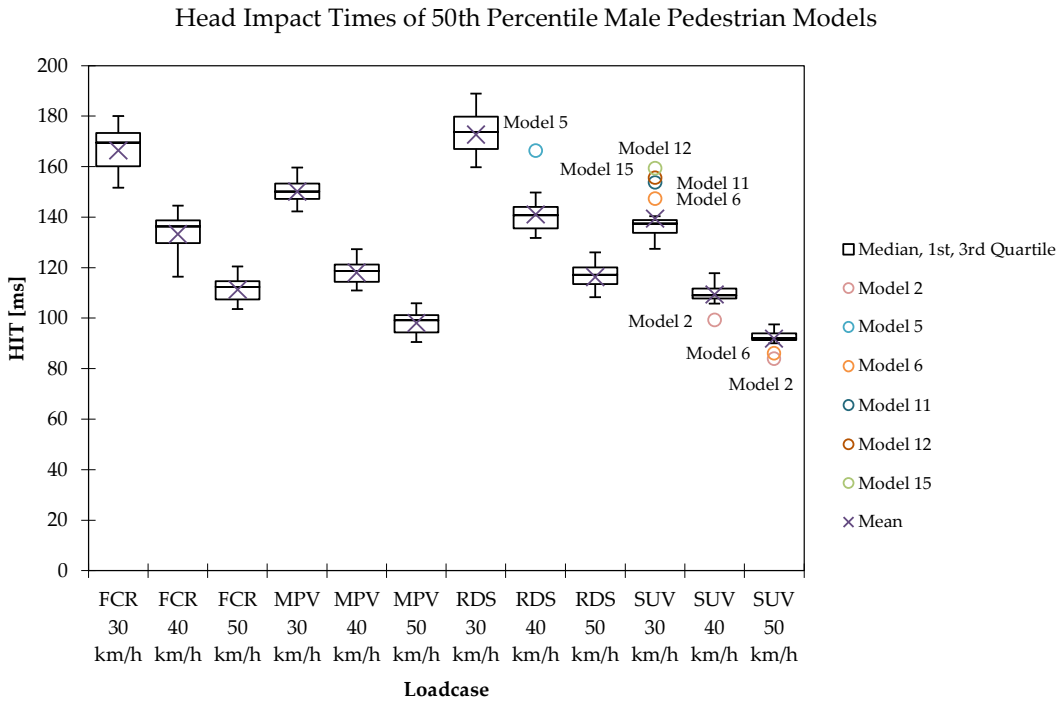

Figure 4: Boxplots of HITs from eighteen different pedestrian simulations for impacts with FCR, MPV, RDS and SUV at 30, 40 and 50 km/h with outliers marked with circles.

In the next step, the outliers were excluded from the dataset that was used to define the tolerances and corridors. The median value from the remaining data was calculated as a reference value. The relative deviation of each result from the reference value per load case was calculated as a percentage and plotted in Figure 5. All datasets with outlying behaviour were marked as unfilled circles and the remaining, consistent datasets that were also used to derive the median / reference value are shown as filled circles. A maximum span of 24% variation of *HIT* compared to the reference value in one loadcase (SUV 30 km/h) was observed in the dataset for all the results provided. Pedestrian Model 2 showed smaller *HIT*s than the consistent models in most of the load cases. For the other outlier models, no clear trend could be detected. While they tended to have smaller *HIT*s for family cars, higher *HIT*s were observed for the SUV impacts at 30 and 40 km/h.

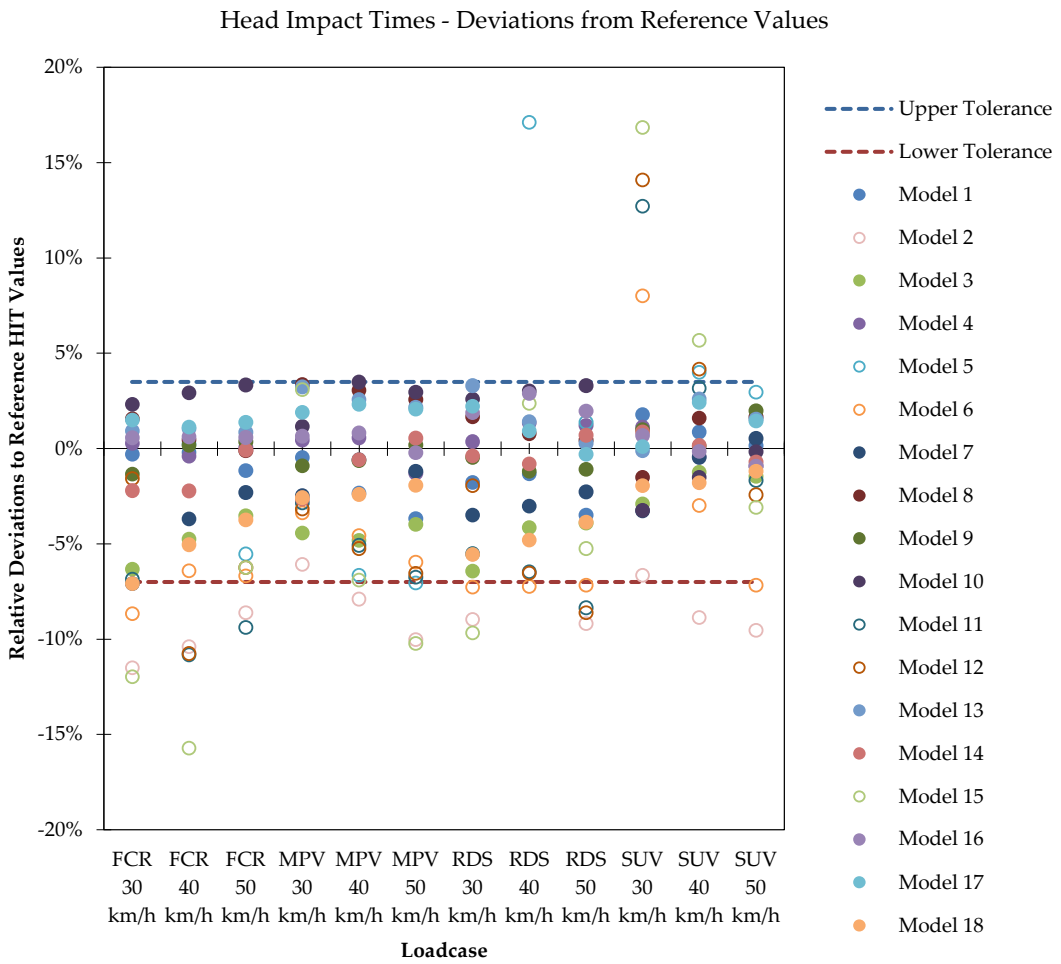

Figure 5: Deviation from reference HIT values of the eighteen different datasets in percent for all twelve load cases (FCR, MPV, SUV, RDS at 30, 40 and 50 km/h).

The maximum and minimum relative deviations within the consistent datasets from the reference value were +3.5% (Model 10 for impact with MPV at 40 km/h) and -7% (Model 18 for impact with FCR at 30 km/h), respectively. These values were chosen as upper and lower allowed tolerance values for the current certification procedure [12]. The reference values together with the derived upper and lower boundaries for the certification procedure are summarised in Table 1.

Table 1.
Reference HIT values and upper and lower boundaries for the certification procedure.

HIT [ms]	**FCR**			**MPV**			**RDS**			**SUV**		
v [km/h]	30	40	50	30	40	50	30	40	50	30	40	50
Reference value	172.3	138.1	114.3	151.5	120.4	100.8	176.9	142.1	119.3	136.5	109.0	92.9
Maximum value (+3.5%)	178.4	143.0	118.4	156.9	124.7	104.4	183.1	147.1	123.5	141.3	112.9	96.2
Minimum value (-7%)	160.2	128.4	106.2	140.8	111.9	93.7	164.5	132.1	110.9	126.9	101.3	86.3

Trajectories

When analysing the trajectories, it was observed that Models 2 and 15 were also outliers in terms of the initial location of the head CoG. They are shown in red in Figure 16 and Figure 6. The initial posture of the head CoG was significantly lower than that of the other models (1635 mm and 1638 mm, respectively, while the median value was 1680 mm and 1.5 *IQR* was 10 mm). They were even beyond the 95% interval of the mean value ± 2 times the standard deviation (1644-1714 mm).

The head CoG of Model 14 was initially located at 1714 mm and, therefore, higher than the median value ±1.5 *IQR*, but fell within the 95% interval. It was maintained in the data sample, since it showed no outlying behaviour in terms of its *HIT*, i.

The minimum and maximum values for each time step were derived in the x and z-directions ($x_{min/max}$ *and* $z_{min/max}$). All models that displayed outlying behaviour in terms of their *HIT*s were excluded prior to creating the corridor. The corridors shown in Figure 6 are exemplary for the 40 km/h impact with the FCR and were derived by connecting the coordinates $[x_{min}(t_n) \quad z_{min}(t_n)]$ for the ascending trajectories (HC, T12) and $[x_{min}(t_n) \quad z_{max}(t_n)]$ for the descending trajectories (AC), as shown in Figure 7. The thick black line in Figure 6 shows the corresponding corridor that was created. Each colour represents the results of one pedestrian model.

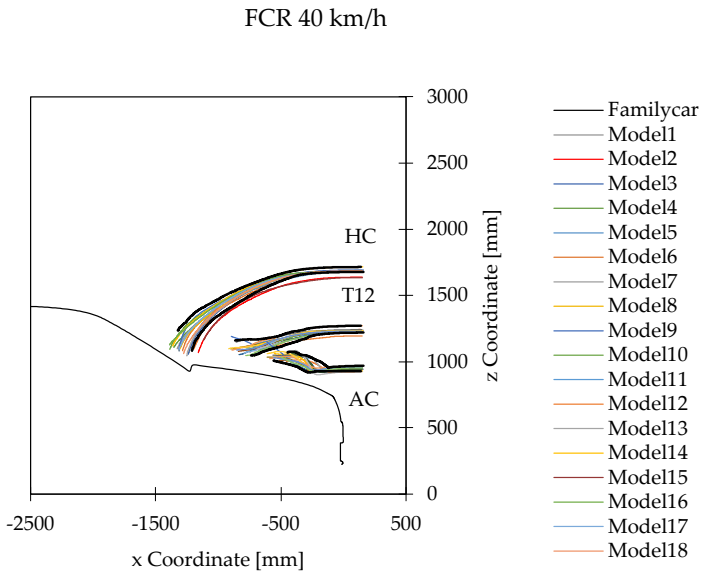

Figure 6: Corridors (black line) for trajectories for z as a function of the x trajectory relative to the vehicle coordinate system for the FCR impact at 40 km/h.

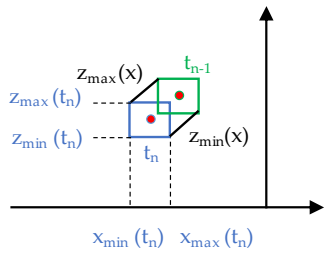

Figure 7: Relationship between time-dependent and x-trajectory-dependent corridors.

As timing is essential for the assessment of the deployable systems, a time dependent approach was finally chosen. This means the coordinate of the analysed reference point (shown as a red point in Figure 7) must lie within a box extending from x_{min} to x_{max} and z_{min} to z_{max} (shown as blue and green boxes in Figure 7 for two different time steps) at each time step. The resulting corridors for z and x as a function of time are shown in Figure 8-Figure 13 as black dashed lines.

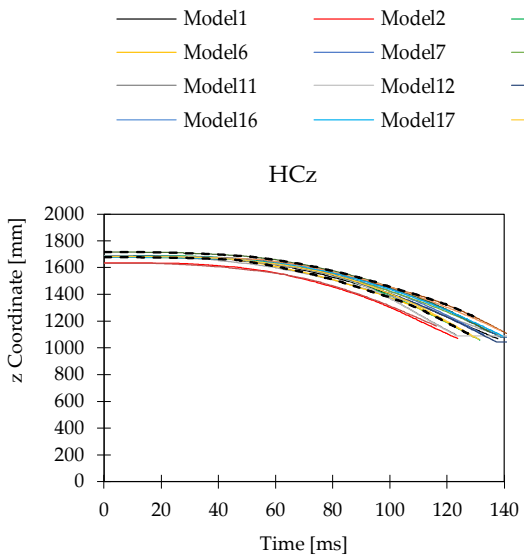

Figure 8: Corridor for the z trajectory as a function of time (black dashed line) for Head CoG for FCR 40 km/h load case.

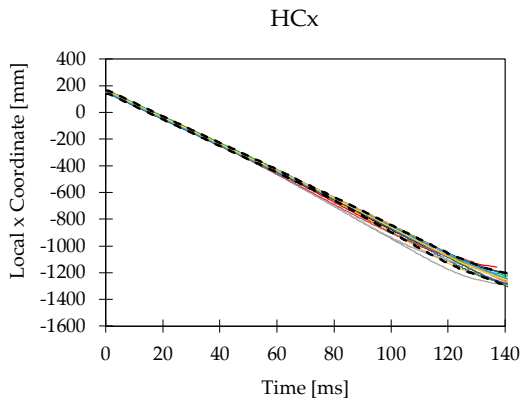

Figure 9: Corridor for the x trajectory as a function of time (black dashed line) for Head CoG for FCR 40 km/h load case.

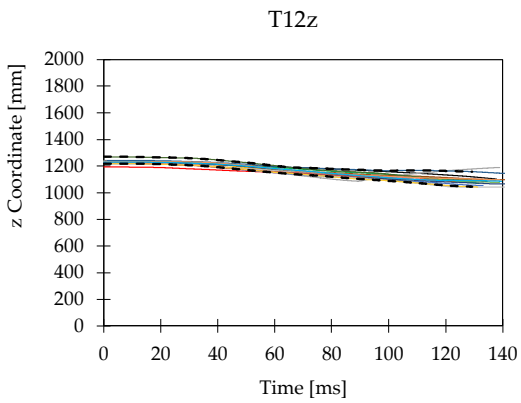

Figure 10: Corridor for the z trajectory as a function of time (black dashed line) for T12 for FCR 40 km/h load case.

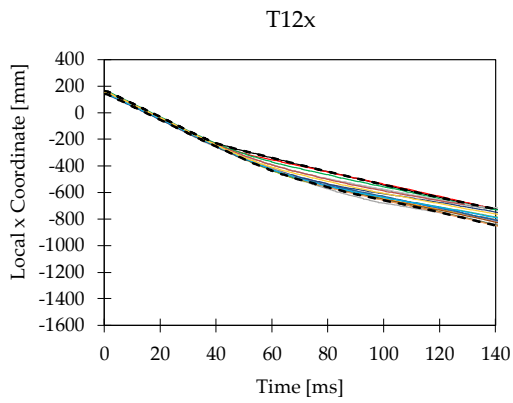

Figure 11: Corridor for the x trajectory as a function of time (black dashed line) for T12 for FCR 40 km/h load case.

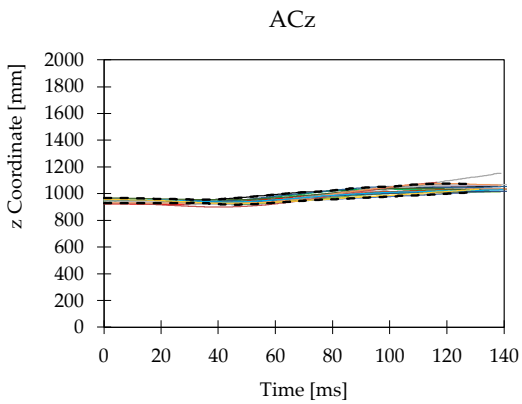

Figure 12: Corridor for the z trajectory as a function of time (black dashed line) for centre of acetabuli for FCR 40 km/h load case.

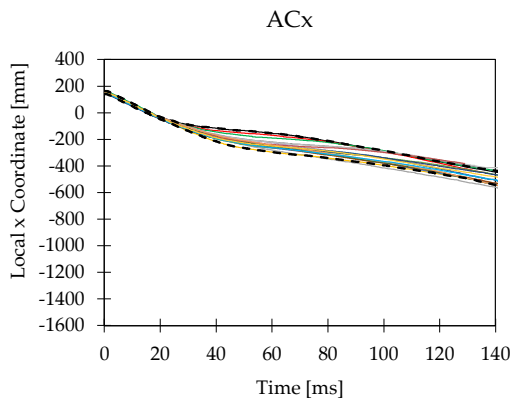

Figure 13: Corridor for the x trajectory as a function of time (black dashed line) for centre of acetabuli for FCR 40 km/h load case.

As shown in Figure 8, Models 11 and 12 (already defined as outliers because of their *HIT*s – shown in grey) fell outside the z corridor towards the end of the simulation. The responses of the other fourteen pedestrian models remained inside the corridors. The corridors for all the load cases can be found in the Appendix.

Contact Forces

Figure 14 shows the resultant total contact force (unfiltered) observed between the pedestrian and GV using the varying HBMs and varying codes, for the 40 km/h impact with the generic FCR model. At around 130 ms the head is impacting the rigid windshield, which is why the forces are increasing drastically. All results for which *HIT*s or trajectories showed outlying *HIT* behaviour are shown in grey. Additionally, the red and orange lines (Models 1 and 3) were also removed, as they showed significantly higher first peaks compared to those in the other models. The corridors, shown as black dashed lines, represent the minimum and maximum values of the contact forces of the remaining consistent models as derived at each time step.

The final corridors for all load cases are shown in the Appendix. Code-specific issues were identified when analysing the contact forces, which is why the contact force corridors are used for monitoring purposes only at the current stage.

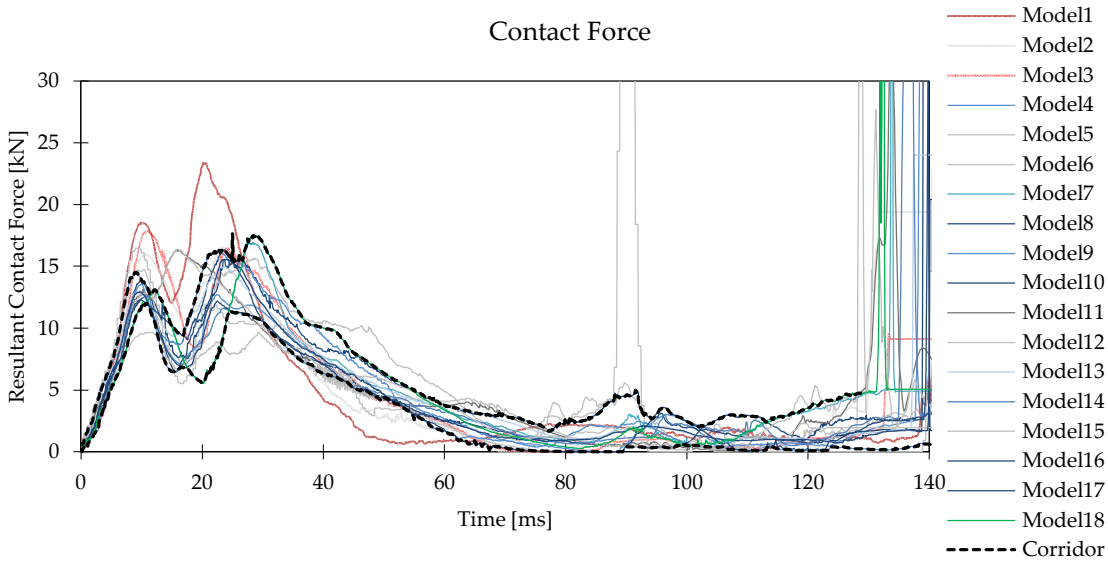

Figure 14: Total resultant contact forces between vehicle and pedestrian models for all submitted results and the derived corridors for a 40 km/h impact with an FCR.

DISCUSSION

Analysed output

A cross-check with the head acceleration in the resultant and global z-directions was performed to see if the time of the head impact had been determined correctly. Whenever the maximum resultant head acceleration was observed before the derived time *H* of head contact, a manual check was performed by examining the animated results. In some cases, this discrepancy was caused by the fact that a direct contact between the head and GV was avoided, as the arm was located between head and GV, leading to high accelerations in the head, but no measured contact force between the head and GV. In these cases, the applied definition led either to no identifiable, or a very high *HIT*.

Three approaches could be applied to deal with this issue:

1. The time *H* could be defined as the time when the head contacts the arms and at the same time the arms contact the vehicle
2. The time *H* could be defined as the time of maximum head acceleration
3. The contact between arms and head could be disabled in such cases.

Approach 1 leads to significantly lower *HIT*s compared to those obtained in simulations with no contact between arms and head and, therefore, leads to less comparable results. Approach 2 can lead to misleading results, as multiple peaks in the head accelerations were observed in some simulations. When the head of the HBM

contacts the shoulder, this can lead to even higher acceleration than if it contacts the bonnet. For these reasons, approach 3 was chosen as it allowed an automatic analysis of *HIT* to be performed and the most readily comparable results to be obtained.

To cover the body kinematics that were relevant for the chosen assessment focus, the trajectories for the head CoG (HC), centre of T12 and the centre of *acetabuli* (AC) were considered as the final reference points and corridors were defined for these: The location of the head is obviously important for the assessment of deployable system because the wrap-around distance and HIT are important outputs for the assessment simulations. AC and T12 enable an analysis of the hip and the torso kinematics, which are important for the evaluation of the deflection due to the body load and for avoiding implausible full-body kinematics. The reference point AC tends to be close to the CoG of the full-body, and the CoG of the torso is located between AC and T12.

Furthermore, T12 and AC together were shown to be indicators that could effectively be used to identify the time when the curvature of the spine started to change its direction. The spine kinematics could be separated into two phases as shown in Figure 15. In the first phase, the pelvis moved away from the head and the upper torso as it was accelerated by the vehicle impact, while the upper torso and head remained in place due to their inertia. The spine posture at 66 ms showed the maximum spine curvature for this load case (FCR impact at 40 km/h) as the pedestrian wrapped around the vehicle. The head and upper torso then were pulled downwards and the spine was straightened, before its curvature changed into the other direction prior to the head impact at 140 ms. This is clearly visible when examining the figures that had fixed pelvises on the bottom of Figure 15 showing the skeleton of THUMS v4.02 in simulations with the GV FCR model in LS-DYNA: In phase 1, T12 is located on the left side of AC, while it is located on the right side in phase 2. The observed kinematics are in accordance with movement patterns seen in PMHS tests [13].

Phase 1 **Phase 2** **Head Impact**

Full-body kinematics (initial position in the background) in the global coordinate system.

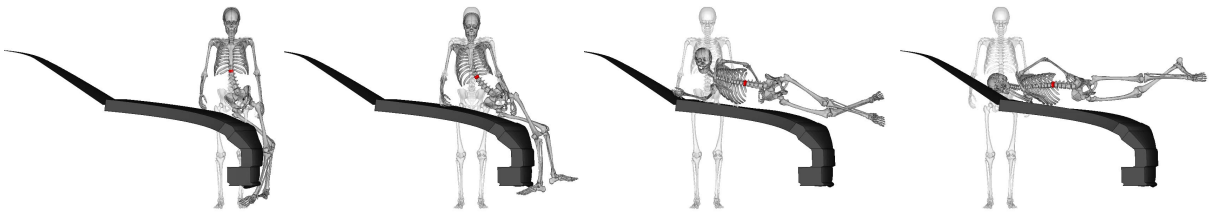

Spine kinematics relative to fixed pelvis coordinate system.

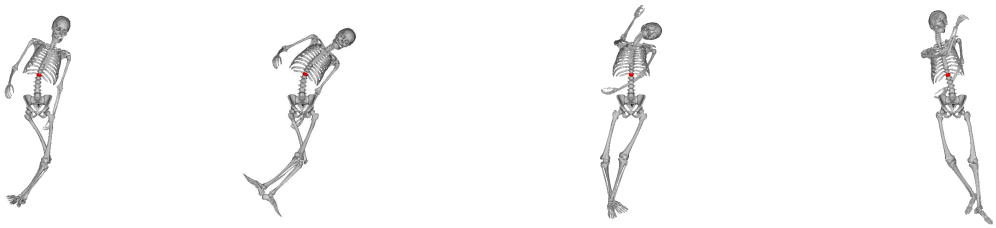

42 ms 66ms 118 ms 140 ms

Figure 15: Kinematics of the spine for an impact with the generic FCR model at 40 km/h relative to the global and a local pelvis coordinate system (T12 shown in red).

The trajectories of the lower extremities were not relevant for the assessment of active bonnets and, therefore, were not included.

Alternative corridor definitions

To define the corridors for the certification procedure, several approaches were taken into account. As a first approach, the method described in the SAE norm J2868 [14] was applied, defining the corridor as a percentage of the path length based median reference trajectories. In this approach, the path length at each time step is derived from the median x and z coordinates for each reference point as a first step. A tolerance of +10% and -5% of the path length is added to the median trajectory, resulting in the corridors shown in Figure 16. As the corridor for the head trajectory was much wider than the spread observed in the analysed data, the method was rejected.

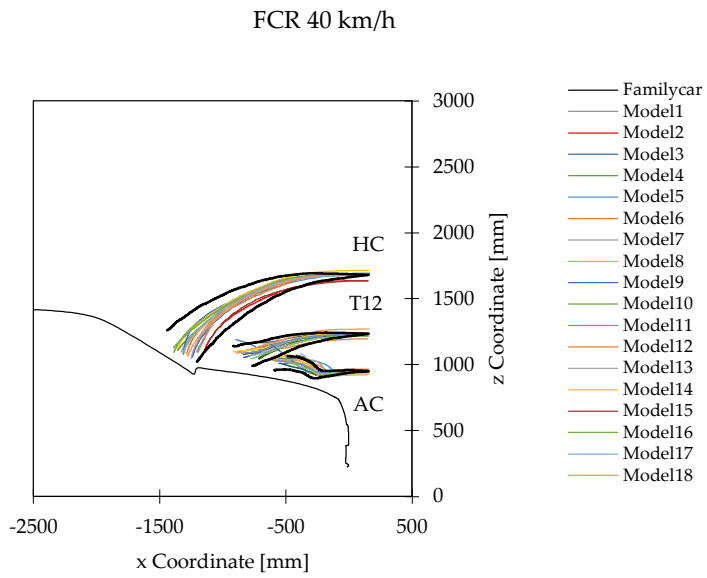

Figure 16: Corridors derived with SAE J2868 approach based on path length for z as a function of the x trajectory relative to the vehicle coordinate system for the FCR impact at 40 km/h.

The corridors introduced in the current paper are based on minimum and maximum values at each timestep. After receiving the first ten certification dossiers, it was realised that even the models used to create the corridors can fall out of the corridor for a short duration (a few milliseconds) and for a few millimetres. Numeric effects can lead to such small deviations, which can be crucial for models that are defining the upper and lower boundary of the corridors. Therefore, an appropriate tolerance was defined for the introductory period. The reference points are allowed to have a maximum deviation of 50 mm to the reference corridors in x- and z-direction. This reference was chosen, as it represents the half the size of the grid used for the head impactor tests. However, at the beginning of the corridor the differences between the models tend to be very small and therefore the additional tolerance tends to be higher in that time period than the maximum differences observed in the simulations.

As a next step, new corridors will be established that are based on another alternative method to avoid this issue, where the mean location at each time step and a corridor based on standard deviations (SD) are derived.

The locations of the reference points in the local vehicle coordinate system (x_i and z_i summarized as c_i) are paired with the time (t_i) as sequences.

$$(t_i, c_i) \text{ for } i = 1, \dots, n. \qquad \text{(Equation 2)}$$

Since multiple datasets are available, there are m sequences of measured values

$$(t_i^r, c_i^r) \text{ for } r = 1, \dots, m \text{ and } i = 1, \dots n_r \qquad \text{(Equation 3)}$$

where a mean of c over r is of interest at each t_i. Subsequently, only sequences are considered which have the same time resolution, but they might stop at different lengths, so n_r can be different for each r. To simplify notation, it is further assumed that the sequences are ordered by their length i.e. $n_1 \geq n_2 \geq \cdots \geq n_m$. The number of sequences that have values for an index i will be denoted as m_i. So m_i equals m for $i \leq n_m$ but it might be smaller than m for $i > n_m$. Let $\bar{n}$ be the longest sequence length for which all sequences have values i.e. $m_i = m$ for $i \leq \bar{n}$ and $m_i < m$ for $i > \bar{n}$. If all sequences have the same length, the mean can be calculated by simply taking the mean over all y-values for each x-value, that is

$$c_i^{mean} = \frac{1}{m}\sum_{r=1}^{m} c_i^r. \qquad \text{(Equation 4)}$$

If the sequences have different lengths, this approach can be modified to

$$c_i^{mean} = \frac{1}{m_i}\sum_{r=1}^{m_i} c_i^r. \qquad \text{(Equation 5)}$$

However, this will lead to "jumps" when a sequence ends. In the following, a method will be outlined to calculate a mean that avoids these "jumps". As long as there is data for all sequences, the usual mean will be used i.e.

$$c_i^{mean} = \frac{1}{m}\sum_{r=1}^{m} c_i^r \text{ for } i \leq \bar{n}. \qquad \text{(Equation 6)}$$

To calculate the mean for $i > \bar{n}$, a mean of the changes of the c is used. Let $\Delta c_i^r = c_{i+1}^r - c_i^r$ be the difference between two consecutive c in the rth sequence. The mean of these differences can be calculated by a similar formula as the mean of c, as

$$\Delta c_i^{mean} = \frac{1}{m_{i+1}}\sum_{r=1}^{m_{i+1}} \Delta c_i^r. \qquad \text{(Equation 7)}$$

To calculate the mean for $i > \bar{n}$ the previous mean value is updated with this mean difference i.e.

$$c_i^{mean} = c_{i-1}^{mean} + \Delta c_{i-1}^{mean} \text{ for } i > \bar{n}. \qquad \text{(Equation 8)}$$

Casually speaking, the mean moves in the direction of the mean slope. If all sequences have the same length, this approach would lead to the ordinary mean even if $\bar{n}$ would be artificially set to 1.

The upper and lower boundaries of the corridors are then defined at each time step as:

$$c_i^{corridor} = c_i^{mean} \mp 2 * SD_i \qquad \text{(Equation 9)}$$

If $i > \bar{n}$, SD_i is no longer updated and is set to $SD_{\bar{n}}$. The corridors according to this new method (SD based) are compared to the corridors introduced in this paper (Min/Max based corridors) in Figure 17. The advantage of the SD based method is also that the whole dataset can be used and outliers do not have to be sorted out necessarily to define the corridor (however, they will affect the standard deviation). The grey area in the figure shows the additional 50 mm tolerance that is allowed in the current version of technical bulletin. The SD-based corridor lay between this additional tolerance (grey shaded area) and the min/max based corridors and would therefore appear to be a good solution to solve the issues described above. If a higher tolerance is needed for an introduction period, the corridor width can be increased to $\mp 3 * SD$.

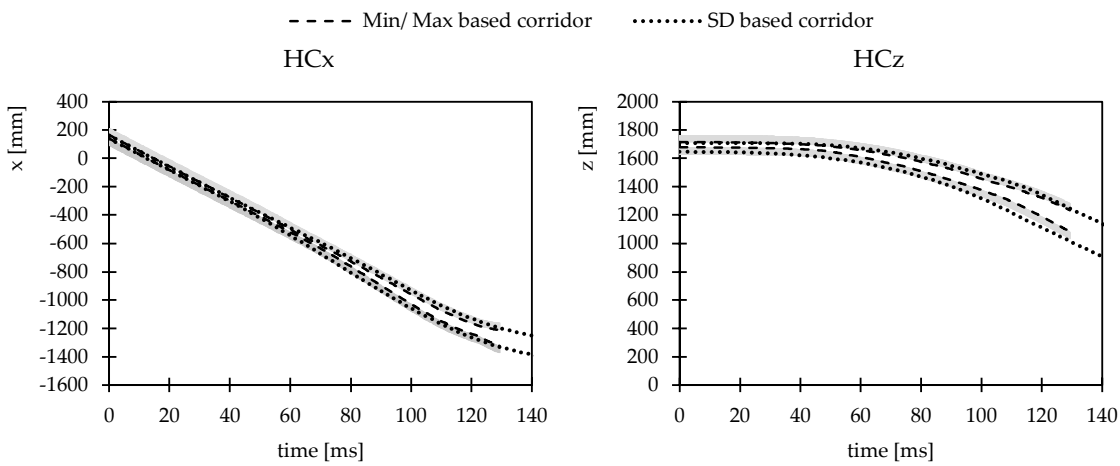

Figure 17: Comparison of time dependent corridors for HCx and HCz.

Comparability of results from HBM simulations

Although GHBMC PS and THUMS AM50 pedestrian models are validated using differing PMHS tests and do not have the exact same anthropometry, the kinematic responses seen were very similar. This was not true for some of the other pedestrian models. It was possible to identify outliers with inconsistent behaviour compared to the majority of results, and these will have to be revised to pass the certification.

Models that showed outlying behaviour for *HIT* also showed outlying behaviour for the trajectories, indicating that the chosen approach, which began with the identification of outliers based on *HIT*s, was appropriate. Two additional outliers were identified for the contact forces that showed comparable behaviour to the other results in the previous analyses. When examining the details, it was observed that discrepancies seem to come from specific output definitions of the contact forces in one FE software package. In the current certification procedure described in TB024 [12] the contact forces are only monitored, which means that the model response does not have to fall within the corridors. The attempt should be made, however, to harmonise the contact force outputs more, with the intention of being able to add this as an additional requirement in the future.

The presented certification procedure does not replace the validation of the HBM in terms of biofidelity. The certification proceeds the validation and allows an HBM in a specific environment to be used as a "virtual test device" for a specific assessment focus (in this case, the kinematic-based assessment of deployable systems). When performing any revisions of the Human Body Models, validations also have to be repeated. While the HBM has to be morphed to the anthropometry of the PMHS to perform a proper validation, reference anthropometries are needed for assessment purposes.

Certification procedures are important prerequisites for virtual testing, as they enable users to determine whether the response of a specific virtual test device in a specific environment answers a specific question and provides a comparable response. Within the certification procedure the response of the model is compared to reference simulations using the harmonized setup, target posture and harmonized anthropometry that should be also used for the final assessment simulations.

The certification procedure has been developed to provide evidence that the pedestrian model leads to comparable results within specified tolerance levels when it is applied in a harmonised setup (this is very similar to the setup that is used for the subsequent assessment). This is required to ensure that the variations in the results fall within an acceptable range. An alternative approach could also be taken to solve this issue: A virtual testing lab performs assessment simulations with the same pedestrian model in the same code for all kinds of cars. Still, once more than one test lab is performing the simulations, or more than one code is used, comparability would be unknown without a certification procedure.

The developed procedure allows users and evaluators to identify user errors when setting up the simulations and to find compatibility problems with FE solver versions. Furthermore, the certification can be used to check the sensitivity of the HBM when control settings have to be changed to comply with the full FE vehicles. The certification procedure can help to increase awareness of the fact that small changes can imply significant effects on the HBM simulation results and that precautions are needed as a result. It can be also used by HBM developers to check the robustness of their models.

The introduced certification procedure is only applicable to kinematic-based assessments. The comparability of injury metrics, and especially strain-based injury metrics, is not addressed. First of all, the kinematics and validations have to be harmonised. Once this has been achieved, similar methods could be applied to compare other metrics for varying models with different setups and codes.

The corridors and tolerances were defined using current state-of-the-art HBMs. No active pedestrian models were covered. The corridors and tolerances are based on biofidelic models, but should not be understood as biofidelity corridors. The corridors will need to be revised when significant changes in the state of the art of HBMs occur and biofidelity significantly improves compared to the current status (e.g. due to newly available test data).

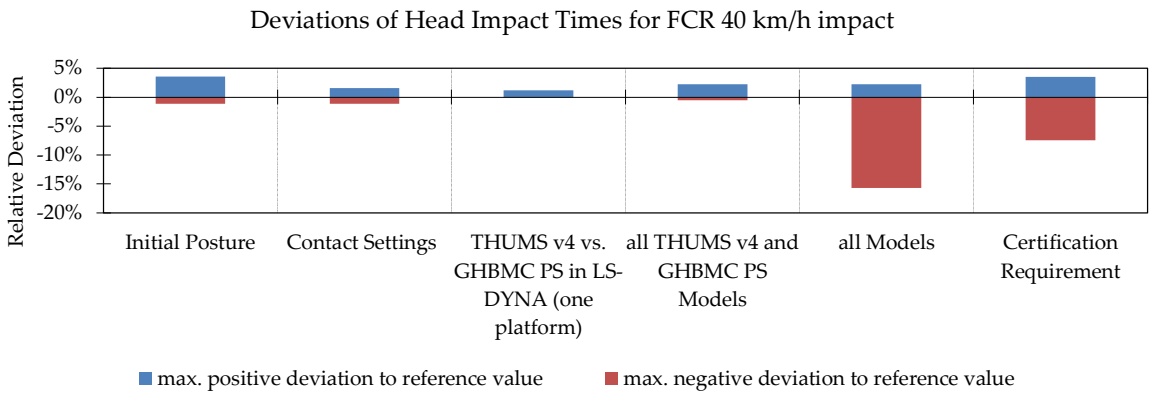

Figure 18 shows the deviations among the *HIT* resulting from different variations for one exemplary load case, the family car impact at 40 km/h, as this is the only load case where results for all variations were available: Due to the harmonised simulation protocol that was introduced in [10], it was possible to narrow down the differences between two models in one FE code and on one platform in terms of *HIT* from 4.7% to 1.2% for this load case. A total variation of 2.75% was observed from the results received with the two models THUMS v4 and GHBMC PS when including the external simulations performed in different codes by different institution.
Without a certification procedure, the models that were listed within TB013 were showing a variation of up to 18% within the FCR 40 km/h load case. Using the current version of the certification procedure results in a decrease in these differences by allowing a maximum of 10.5% variation.
Asymmetric tolerances for the HIT values were defined: A greater amount of negative deviation was accepted, because it represents the worst case for the assessment of the deployable system, while a too high *HIT* was unacceptable. The aim for the future should be to find a way of narrowing down the corridors in when harmonisation in the HBMs is progressing.

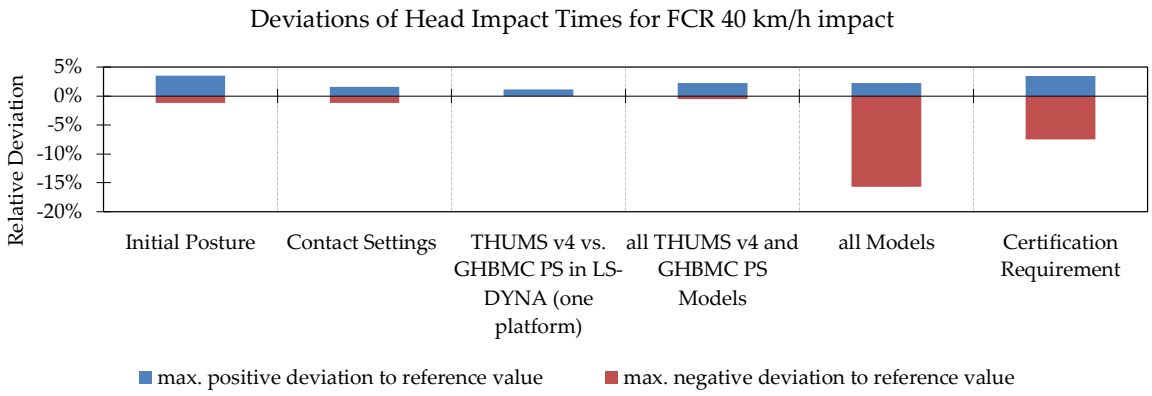

Figure 18: Relative deviations of HITs to reference HIT (138.1 ms) for the 40 km/h impact with generic FCR models.

The benefit of the certification procedure becomes even more obvious when examining the maximum differences observed throughout all load cases and all eighteen sets of analysed results. As shown in Figure 19, the sum of the absolute maximum deviations observed throughout all simulations made up a total of 33% (maximum of 24% within one load case). Due to the certification requirements, this is more than halved to a maximum of 10.5%. The critical positive deviation compared to the reference value, which led to higher *HIT*s, decreased from 17% to 3.5%. The results of the THUMS and GHBMC PS models – in all codes – did not need the full tolerance. Their results fell within a 6.5% range throughout all load cases.

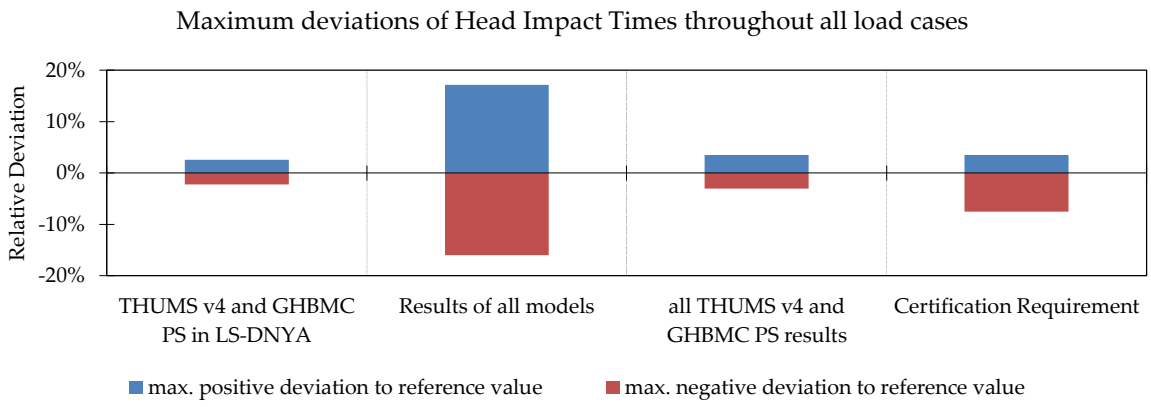

Figure 19: Relative deviations of HITs to reference HITs throughout all twelve load cases.

Outlook

As the 6yo child tends to be the most critical size when it comes to the evaluation of HIT, the response of those models was analysed as a next step. Some additional challenges for the child models were identified compared to the adult models: No full-scale PMHS tests are available with children. Furthermore, there are different kinds of child models available. While the adult models tend to differ only in terms of geometry, there are child models available that have been developed from scratch, such as the PIPER models [15], or some child models that belong to a family, but have been significantly adapted (e.g. material models), to better replicate a child, such as the GHBMC child model [16]. Another challenge is that the anthropometries among the child models differ more than the AM50 models.

The results of simulations with different child models have again been collected, to address those challenges by aiming to establish a second set of reference corridors for the pedestrian models in the size of the 6yo.

The work is still in progress, which is why the results are not included in the current paper. In contrast to the AM50 models, no clear outliers were identified. The preliminary results based on different GHBMC models, THUMS models, PIPER models and one Simcenter Madymo™ model are shown in Figure 20. Summarising all twelve load cases, the maximum spread of HIT values was -12% and +10% and the average spread -7.2% and +6.7% to the mean value derived for each load case, with the same methodology as for the AM50 model. The aim for the future should be to find a way of narrowing down these spreads.

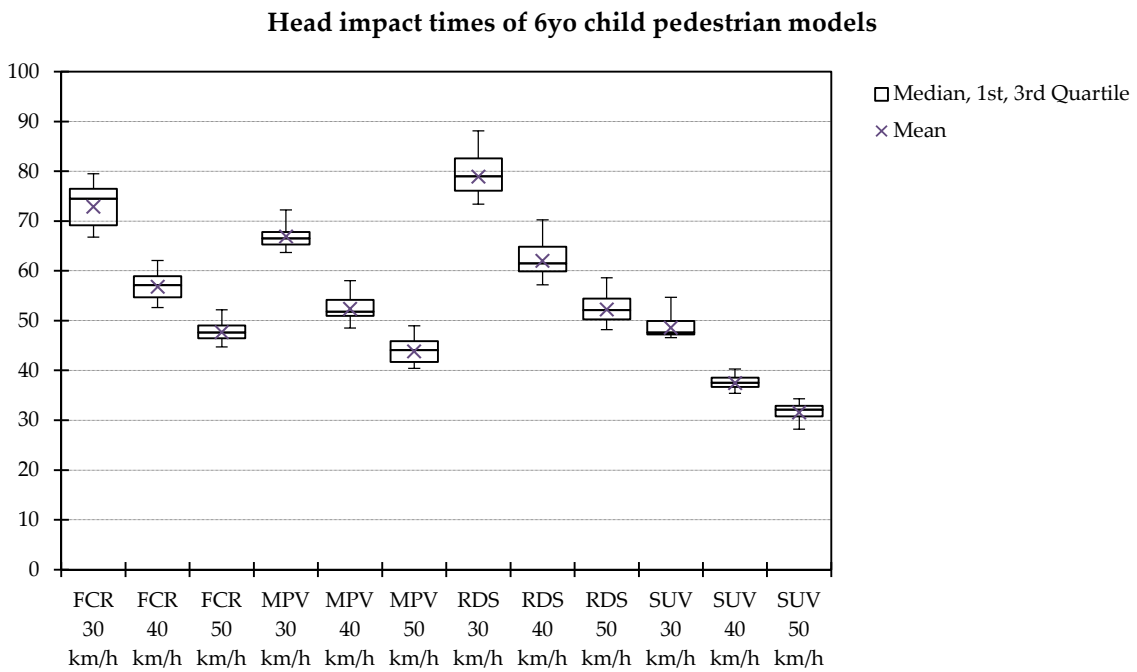

Figure 20: Preliminary HIT values for simulations with 6yo child pedestrian models shown as boxplots.

CONCLUSION

The paper describes the first certification procedure that enables an objective standardised comparison of the kinematic response of various numerical pedestrian models in multiple codes. The procedure was adopted by Euro NCAP and published as Technical Bulletin 024 in January 2018.

When eighteen different results for the twelve reference load cases – performed by different institutions with different HBMs in different FE software packages – were obtained according to the protocol, outliers were identified. The relative amount of deviation among the kinematic-based assessment results was drastically reduced when these were eliminated.

The newly developed certification procedure for HBMs limits the amount of variation allowed for the simulations in the reference load cases to the amount of variation that was observed within the consistent reference simulations (without outliers). The comparability of kinematic-based assessment was, therefore, drastically improved. While, for example, the head impact times in the initial data set varied by up to 24%, the procedure limits the variation to a maximum of 10.5%. This means that the relative deviation of results was more than halved for this output, which is essential for the Euro NCAP assessment of deployable systems.

Certification procedures for numerical models are an important prerequisite to enable virtual testing with numeric pedestrian models for the assessment of safety features. The developed certification procedure provides confirmation that a specific pedestrian model within a specific environment, solver version and specific simulation settings leads to comparable kinematic results relevant for the assessment of deployable systems. Inconsistent pedestrian models, incompatibilities with control settings and user errors can be identified and addressed.

ACKNOWLEDGEMENT

The study is part of the CoHerent Project funded mainly by Euro NCAP. The authors would also like to thank ACEA TF□P for financial support.

The authors would like to thank all the experts who took part in the CoHerent meetings for their inputs and especially all the participants who provided their results for developing the corridors. All the contents of the presented work, except the data from the data providers, are made solely at the own discretion of the authors.

The authors also gratefully acknowledge the use of HPC resources provided by the ZID at Graz University of Technology, Austria.

REFERENCES

[1] Euro NCAP, December 2016. Euro NCAP Pedestrian Testing Protocol(8.3); Available from: http://euroncap.blob.core.windows.net/media/25840/euro-ncap-pedestrian-testing-protocol-v83-december-2016.pdf. [February 22, 2017].

[2] Euro NCAP, November 2015. Pedestrian CAE Models & Codes. 1st ed.(13); Available from: http://euroncap.blob.core.windows.net/media/21510/tb-013-pedestrian-cae-models-v15.pdf.

[3] Tang J., Zhou Q., Nie B., Yasuki T., Kitagawa Y., 2016. Influence of Pre-impact Pedestrian Posture on Lower Extremity Kinematics in Vehicle Collisions. SAE Int. J. Trans. Safety 4(2):278–88. https://doi.org/10.4271/2016-01-1507.

[4] Chen H., Poulard D., Crandall J.R., Panzer M.B., 2015. Pedestrian Response with Different Initial Positions During Impact with a Mid-Sized Sedan. In: NHTSA, editor. The 24th ESV Conference Proceedings. NHTSA, p. 1–12.

[5] Paas R., Östh J., Davidsson J., 2015. Which Pragmatic Finite Element Human Body Model Scaling Technique Can Most Accurately Predict Head Impact Conditions in Pedestrian-Car Crashes? In: International Research Council on the Biomechanics of Injury, editor. 2015 IRCOBI Conference Proceedings. IRCOBI, p. 546–576.

[6] Watanabe R., Miyazaki H., Kitagawa Y., Yasuki T., 2011. Research of the Relationship of Pedestrian Injury to Collision Speed, Car-type, Impact Location and Pedestrian Sizes Using Human FE Model (THUMS Version 4). In: NHTSA, editor. The 22nd ESV Conference Proceedings. NHTSA, p. 1–13.

[7] Kam C.Y., Kerrigan J., Meissner M., Drinkwater C., Murphy D., Bolton J. et al., 2005. Design of a Full-Scale Impact System for Analysis of Vehicle Pedestrian Collisions. In: SAE, editor. SAE 2005 World Congress & Exhibition. SAE International.

[8] Elliott J.R., Simms C.K., Wood D.P., 2012. Pedestrian head translation, rotation and impact velocity: The influence of vehicle speed, pedestrian speed and pedestrian gait. Accid Anal Prev 45(0):342–53. https://doi.org/10.1016/j.aap.2011.07.022.

[9] Kerrigan J., Arregui C., Crandall J., 2009. Pedestrian Head Impact Dynamics: Comparison of Dummy and PMHS in Small Sedan and large SUV Impacts. In: NHTSA, editor. The 21st ESV Conference Proceedings. NHTSA, p. 1–15.
[10] Klug C., Feist F., Raffler M., Sinz W., Petit P., Ellway J. et al., 2017. Development of a Procedure to Compare Kinematics of Human Body Models for Pedestrian Simulations. In: International Research Council on the Biomechanics of Injury, editor. 2017 IRCOBI Conference Proceedings. IRCOBI, p. 509–530.
[11] Klug C., Feist F., Sinz W., Ellway J., van Ratingen M., 2018. A procedure to compare kinematics of Human Body Models for pedestrian assessments. In: SAE International, editor. SAE Government Industry Meeting 2018.
[12] Euro NCAP, November 2017. Pedestrian Human Model Certification. 1st ed.(TB 024):TB 024, 1-35; Available from: https://cdn.euroncap.com/media/32277/tb-024-pedestrian-human-model-certification-v10.pdf.
[13] Subit D., Kerrigan J., Crandall J., Fukuyama K., Yamazaki K., Kamiji K. et al., 2008. Pedestrian-vehicle interaction: Kinematics and injury analysis of four full-scale tests. In: International Research Council on the Biomechanics of Injury, editor. 2008 IRCOBI Conference Proceedings. IRCOBI, p. 275–294.
[14] SAE International, 14.10.2010. Pedestrian Dummy Full Scale Test Results and Resource Materials. 201010th ed.(J2868). USA.
[15] Peres J., 2018. A Pedestrian Version of the Piper 6 Year Old Child Model. In: International Research Council on the Biomechanics of Injury, editor. 2018 IRCOBI Conference Proceedings. IRCOBI, p. 247–248.
[16] Meng Y., Pak W., Guleyupoglu B., Koya B., Gayzik F.S., Untaroiu C.D., 2017. A finite element model of a six-year-old child for simulating pedestrian accidents. Accid Anal Prev 98:206–13. https://doi.org/10.1016/j.aap.2016.10.002.

APPENDIX

Table 2.
Reference Points

Abbreviation	Long Name	Definition
HC	Head centre of gravity	CoG of all parts of skull, scalp, face, brain, intracranial space, scalp) connected to all nodes of inner cranium (at least 100 nodes)
T12	Centre of twelfth thoracic vertebrae	Centre* of all nodes of vertebral body (as defined in Figure 21) T12; connected to all nodes of vertebral body of T12
ACr	Centre of the right acetabulum	Centre* of all nodes within the concave surface of the right acetabulum as shown in Figure 22, connected with all nodes inside. The sharp edge where the bone changes curvature is selected as boundary, and all nodes inside are picked
ACl	Centre of the left acetabulum	As ACr, but for the right acetabulum
AC	midpoint of the right and left acetabulum centres	The midpoint of the left and right acetabulum centres (ACr and ACl) connected to all nodes of the right and left acetabulum.

* Centre always refers to the node with the averaged coordinates of the nodes that were selected to derive the centre as described in Equation (10).

$$x_c = \sum_{i=1}^{n} \frac{x_i}{n} \qquad y_c = \sum_{i=1}^{n} \frac{y_i}{n} \qquad z_c = \sum_{i=1}^{n} \frac{z_i}{n} \tag{10}$$

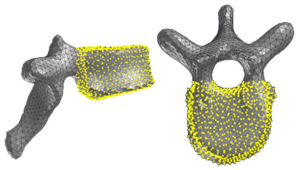

Figure 21. Definition of vertebral body

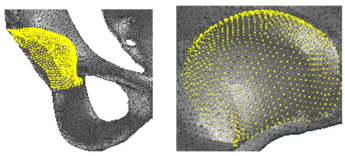

Figure 22. Nodes to derive centre of acetabulum

Table 3.
Keywords for connection of sensor nodes to surrounding structure

Code	Keyword	Recommended Parameters
LS-DYNA	*CONSTRAINED_INTERPOLATE	DDOF = 123456, CIDD = 0, ITYP = 1, IDOF = 123, TWGHTi = RWHGTi = 0
VPS	OTMCO_/	DOFCOD = 111000, IMETH = 0, IELM = 1, ITYP = 0, RADIUS = 0, WTFAC = 1
RADIOSS	/RBE3	I_MODIF = 2 or 3, WTi = 1, TRAROT_REFi = 111111, TRAROT_Mi = 111000
ABAQUS	*MPC	BEAM, NSET1, NSET2

FCR 30 km/h

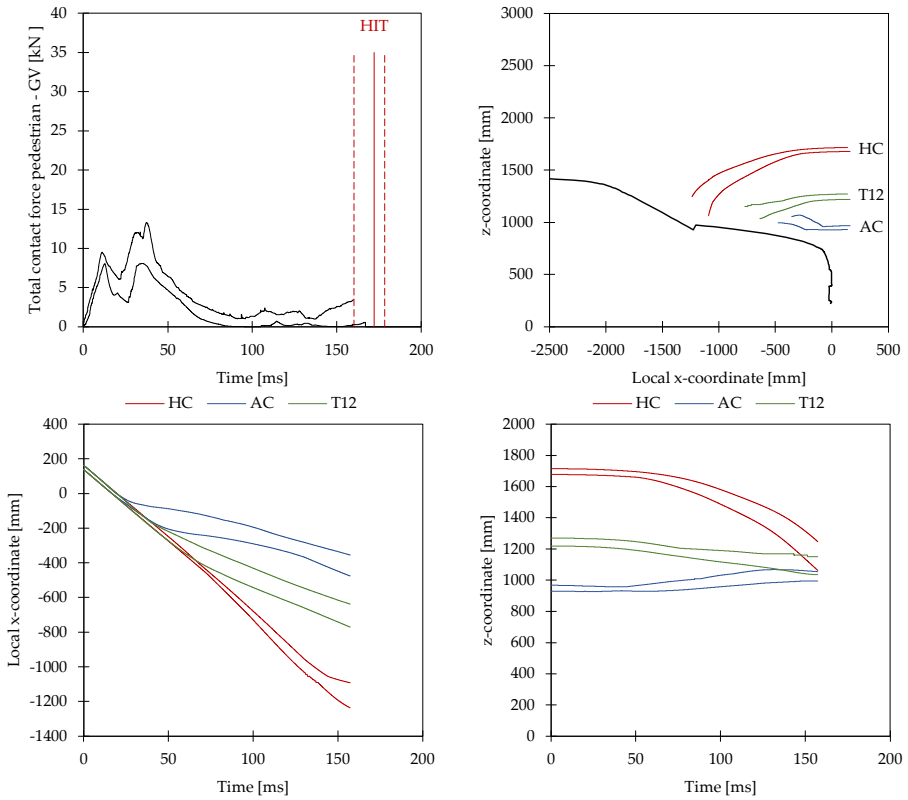

Figure 23. Corridors for impact with generic FCR model at 30 km/h – Reference* HIT = *172.3 ms.

FCR 40 km/h

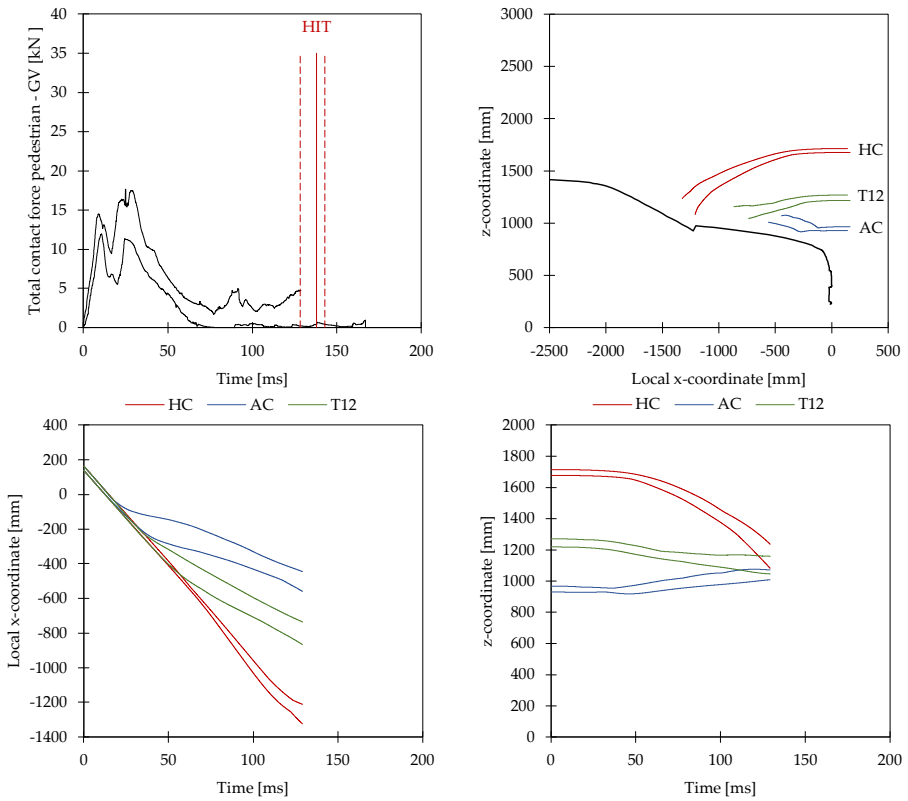

Figure 24. Corridors for impact with generic FCR model at 40 km/h – Reference* HIT = *138.1 ms.

FCR 50 km/h

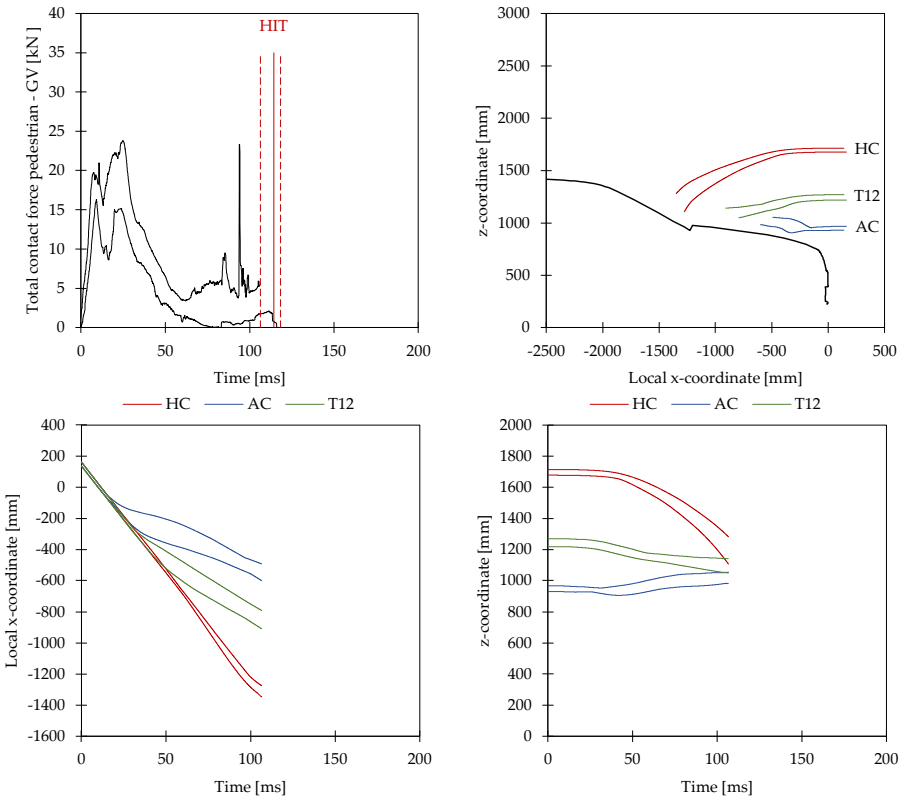

Figure 25. Corridors for impact with generic FCR model at 50 km/h – Reference **HIT** *= 114.3 ms.*

MPV 30 km/h

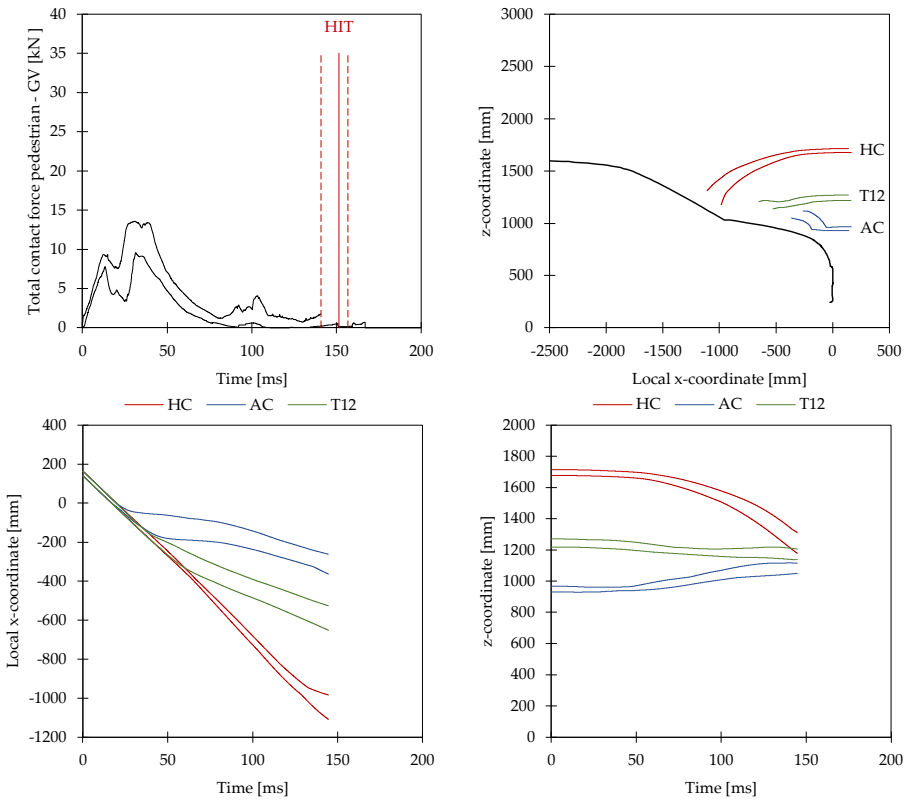

Figure 26. Corridors for impact with generic MPV model at 30 km/h – Reference **HIT** *= 151.5 ms.*

MPV 40 km/h

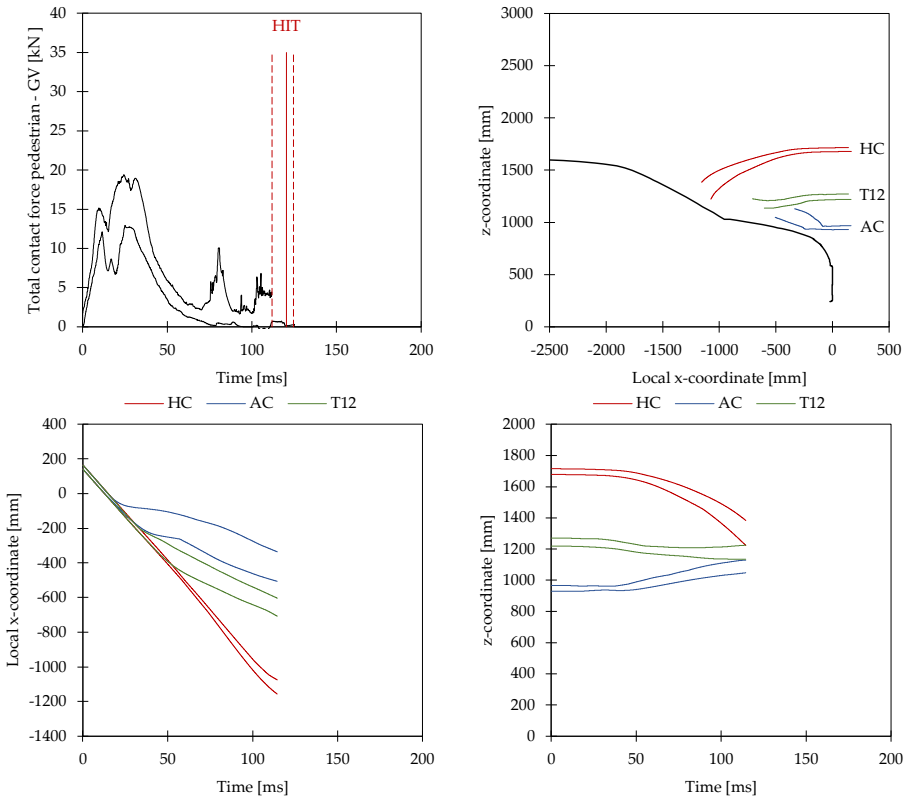

Figure 27. Corridors for impact with generic MPV model at 40 km/h – Reference **HIT** *= 120.4 ms.*

MPV 50 km/h

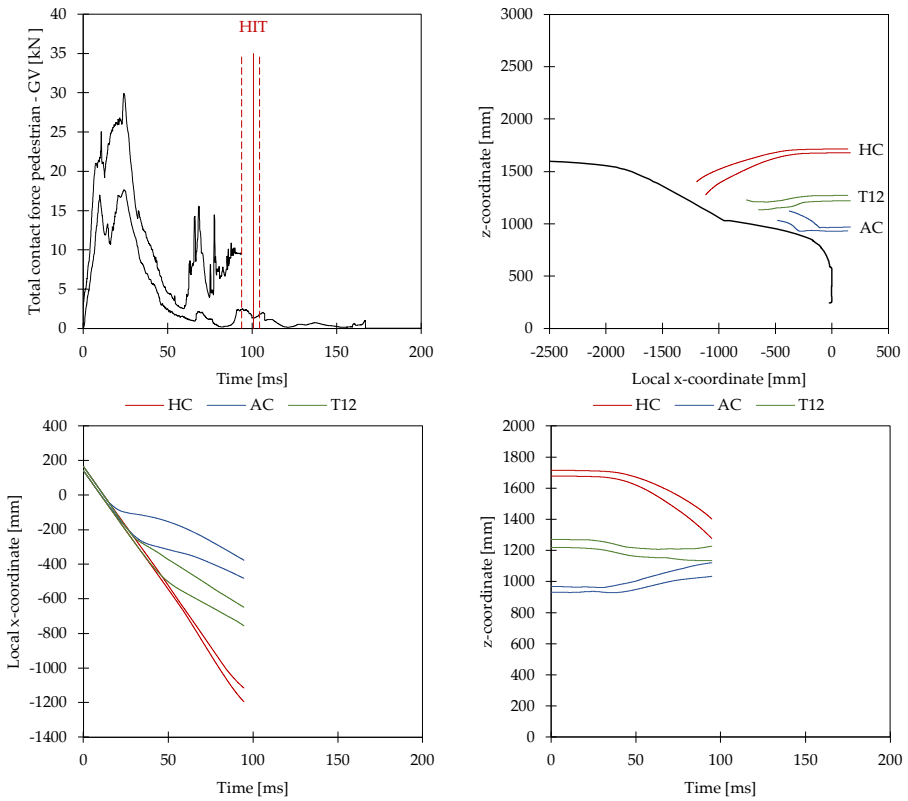

Figure 28. Corridors for impact with generic MPV model at 50 km/h – Reference **HIT** *= 100.8 ms*

RDS 30 km/h

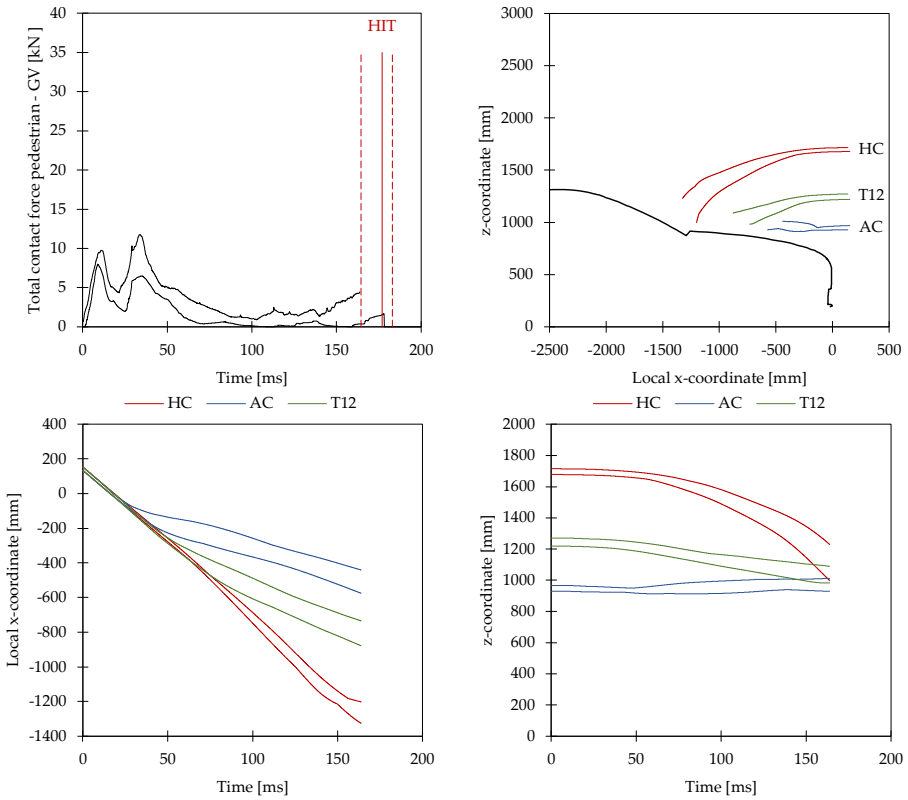

Figure 29. Corridors for impact with generic RDS model at 30 km/h – Reference* HIT *= 176.9 ms.

RDS 40 km/h

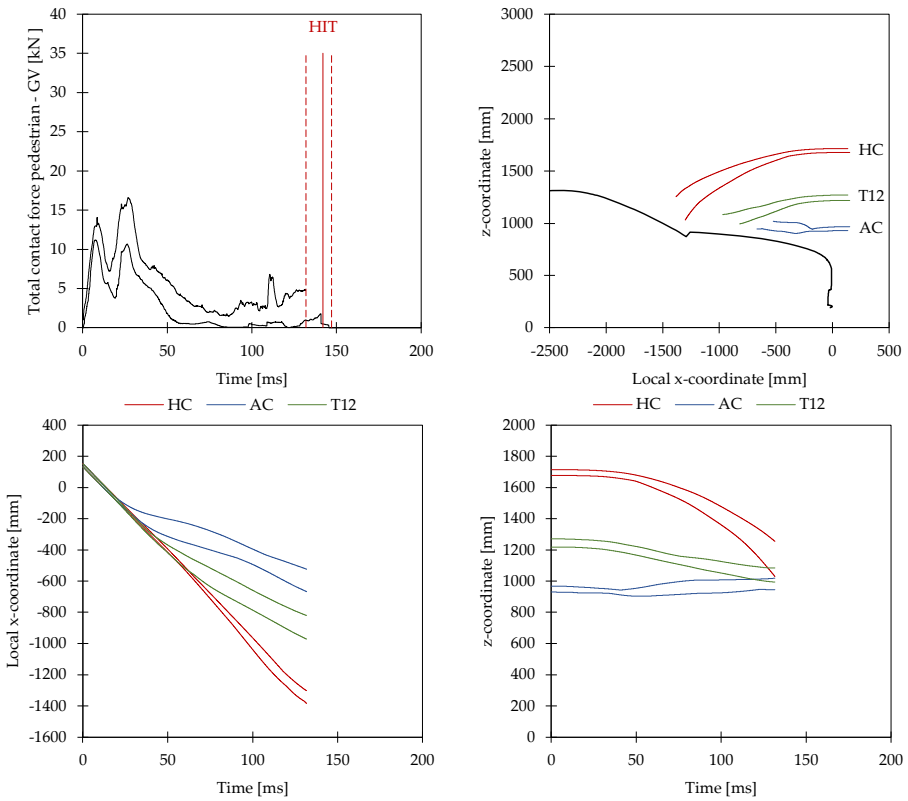

Figure 30. Corridors for impact with generic RDS model at 40 km/h – Reference* HIT *= 142.1 ms.

RDS 50 km/h

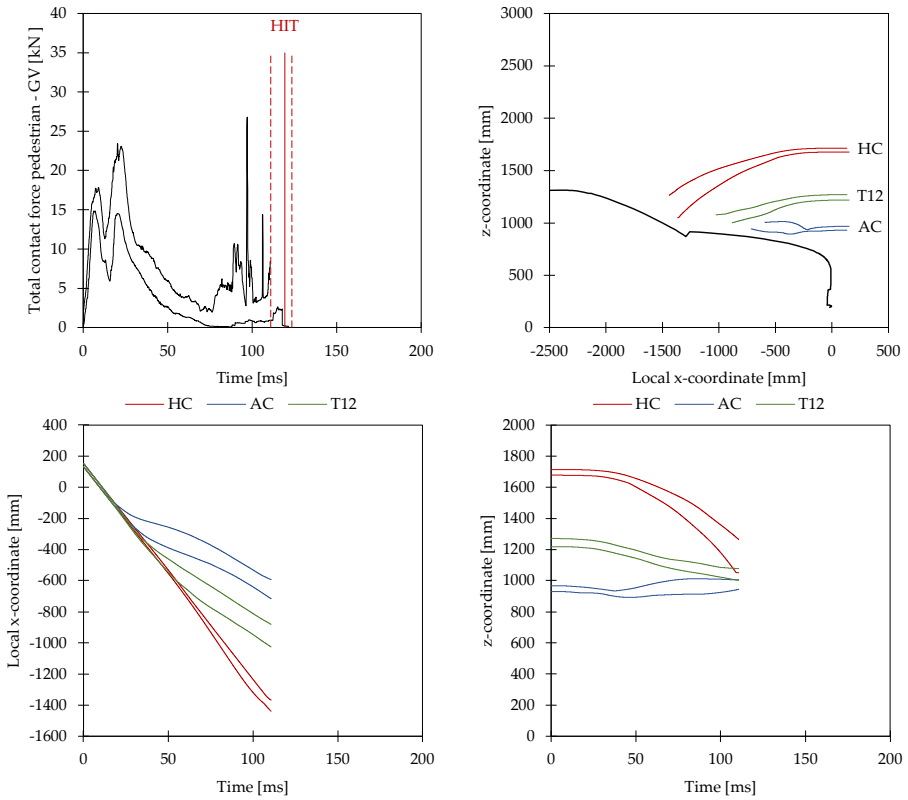

Figure 31. Corridors for impact with generic RDS model at 50 km/h – Reference* HIT *= 119.3 ms.

SUV 30 km/h

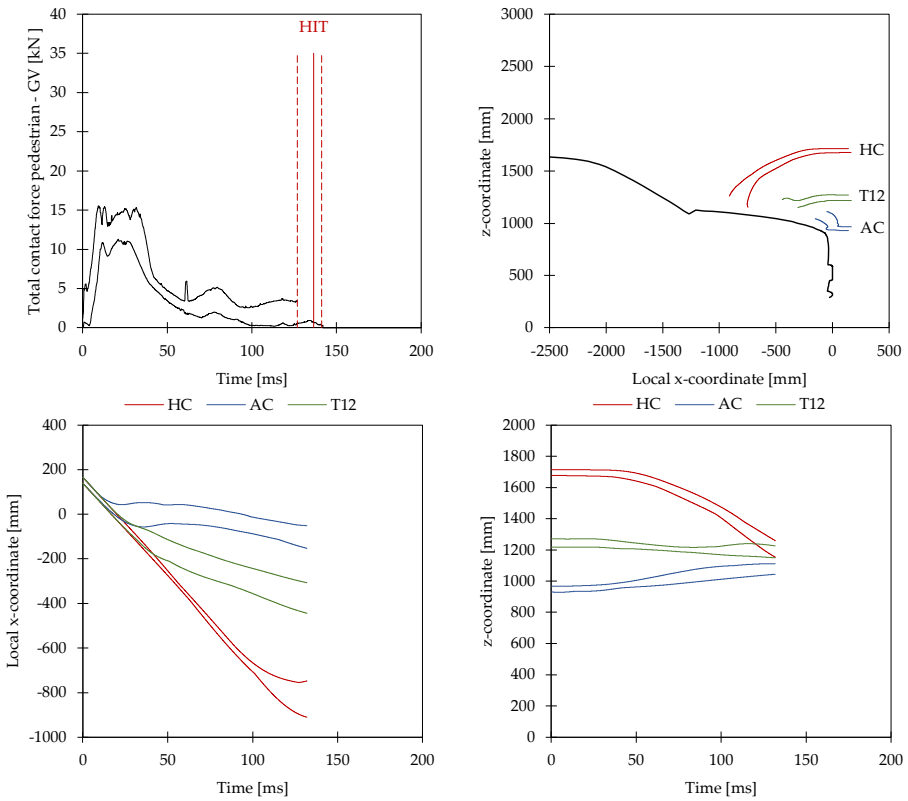

Figure 32. Corridors for impact with generic SUV model at 30 km/h – Reference* HIT *= 136.5 ms.

SUV 40 km/h

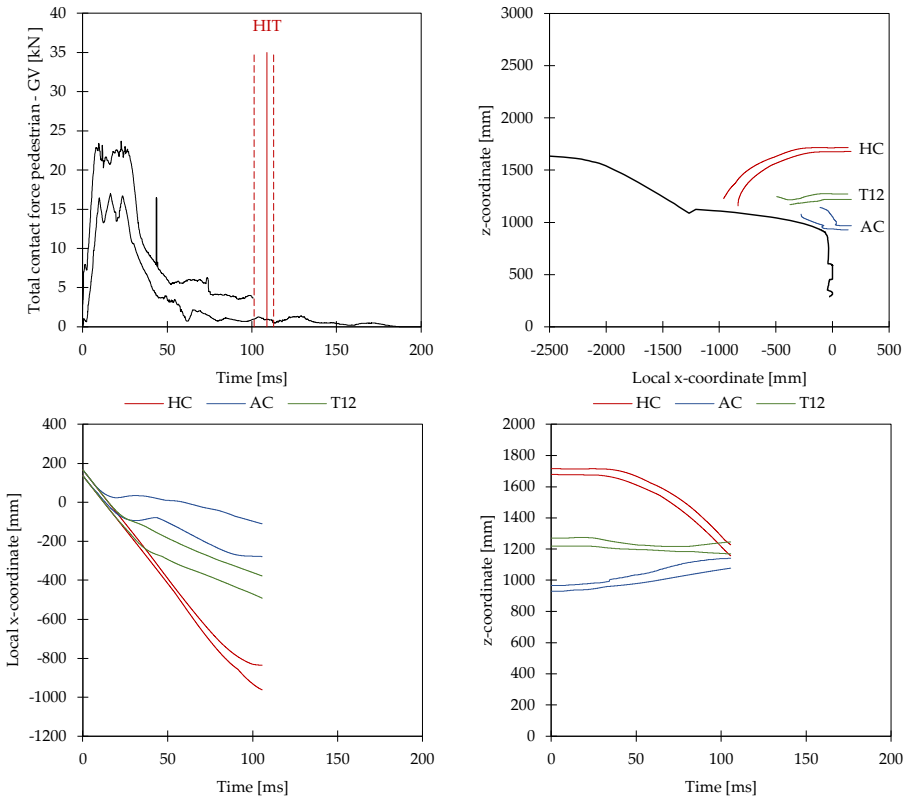

Figure 33. Corridors for impact with generic SUV model at 40 km/h – Reference* HIT = *109.0 ms .

SUV 50 km/h

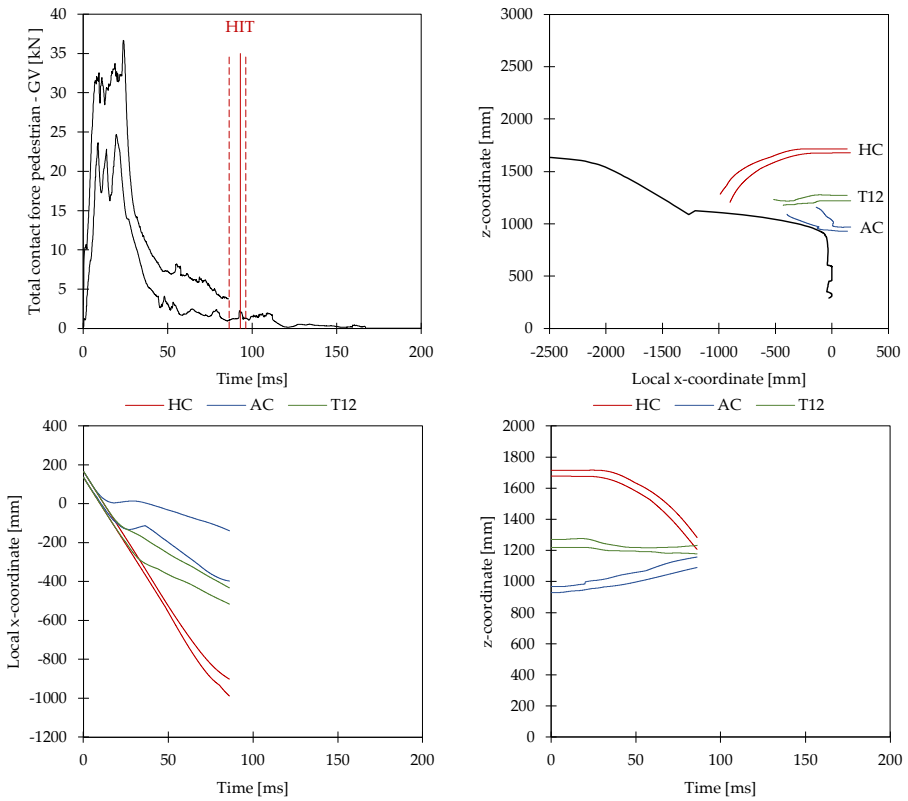

Figure 34. Corridors for impact with generic SUV model at 50 km/h – Reference* HIT = *92.9 ms